

QSAR Study for the Soybean 15-Lipoxygenase Inhibitory Activity of Organosulfur Compounds Derived from the Essential Oil of Garlic

ALEJANDRA B. CAMARGO,[†] EDUARDO MARCHEVSKY,[§] AND JUAN M. LUCO^{*,#}

Laboratorio de Análisis de Residuos Tóxicos, Facultad de Ciencia Agrarias, Universidad Nacional de Cuyo, Alte. Brown 500, Chacras de Coria 5505 Mendoza; and Area de Química Analítica and Laboratorio de Alimentos, Facultad de Química, Bioquímica y Farmacia, Universidad Nacional de San Luis, Chacabuco y Pedernera 5700 San Luis, Argentina

In this study, multiple linear regression (MLR) and partial least-squares (PLS) techniques were used for modeling the soybean 15-lipoxygenase inhibitory activity of a varied group of mono-, di-, and trisulfides derived from the essential oil of garlic. The structures of the compounds under study were characterized by means of calculated physicochemical parameters and several nonempirical descriptors, such as topological, geometrical, and quantum chemical indices. The results obtained indicate that the inhibitory activity is strongly dependent on the ability of the compounds to participate in dispersive interactions with the enzyme, as expressed by the solvent-accessible surface area (SASA) and the average distance/distance degree descriptor (ADDD) index. On the other hand, the high contribution of the lowest unoccupied molecular orbit term (LUMO) in the PLS models derived for the di- and trisulfides suggests that the solute's electron-acceptor capacity plays a fundamental role in the inhibitory activity exhibited for these compounds. Finally, the geometric features as expressed by the shape parameters included in the models indicate a low but not negligible positive contribution of molecular linearity in the enzyme–inhibitor binding. In summary, the developed quantitative structure–activity relationship approach successfully accounts for the potencies of organosulfur compounds acting on soybean 15-lipoxygenase and thereby offers both a guide for the synthesis of new compounds and a hypothesis for the molecular basis of their activity.

KEYWORDS: Multivariate quantitative structure–activity relationships (QSARs); soybean 15-lipoxygenase (15-sLO); garlic; organosulfur compounds (OSCs)

INTRODUCTION

Lipoxygenases (LOs) are a class of widely occurring, non-heme iron-containing oxygenases that can be isolated from animals, higher plants, and fungi (1, 2). LOs contribute to the eicosanoid pathway by the incorporation of dioxygen into 1,4-*cis,cis*-pentadiene containing fatty acids (e.g., linoleic and arachidonic acids) to form hydroperoxy derivatives (3). These enzyme products are intermediates in the biosynthesis of numerous compounds of wide pathophysiological implications in humans, including various inflammatory conditions such as arthritis, psoriasis, and bronchial asthma, as well as immune disorders and carcinogenic processes (4–6). There is also evidence that 15-lipoxygenase is induced in human atherosclerosis lesions (7) and that it is capable of oxidizing low-density lipoprotein to its atherogenic form (8). Currently, three distinct mammalian LOs have been characterized, 5-LO, 12-LO, and

15-LO, which oxygenate arachidonic acid at specific carbon centers (C5, C12, and C15, respectively).

Although plant and mammalian LOs contain about 25% amino acid identity between the two families, their overall structures are very similar, especially in the catalytic domain in the region of the active site (9). Consequently, discovery of new and selective LO inhibitors appears to be an important challenge due to their impact in the treatment of the above-mentioned diseases. With regard to its characteristics and mechanism of action, the LO inhibitors have been classified into four distinct classes: (i) iron-chelating inhibitors, (ii) competitive reversible inhibitors, (iii) inhibitors of the 5-lipoxygenase activating protein (FLAP), and (iv) antioxidative. The structural and mechanistic aspects on substrates and inhibitors of the LO reaction have been reported recently (10, 11).

Garlic (*Allium sativum* L.) has been used worldwide as a food and medicinal plant since ancient times, and many of the beneficial health-related biological effects have been attributed to its characteristic organosulfur compounds (OSCs) (12). The best known and most extensively studied is allicin (diallyl thiosulfinate), the main biologically active compound of fresh

* Author to whom correspondence should be addressed (e-mail jmluco@unsl.edu.ar; fax +54-2652-430224).

[†] Universidad Nacional de Cuyo.

[§] Area de Química Analítica, Universidad Nacional de San Luis.

[#] Laboratorio de Alimentos, Universidad Nacional de San Luis.

garlic juice, which is relatively unstable and decomposes into a variety of OSCs (13).

There is ample evidence that many OSCs found in *Allium* tissue preparations are responsible of various biological activities such as antimicrobial, anticancer, antihypertensive, hypolipidemic, hepatoprotective, and antithrombotic ones (14, 15).

Currently there exist in the market different commercial garlic products, such as powder tablets, macerated garlic oil, and steam-distilled oil, which vary in their physiological activities due to their differences in the type and percentage composition of OSCs.

In an interesting work, Block and co-workers (16) studied the inhibition of soybean 15-lipoxygenase (15-sLO) by using several garlic essential oil preparations to determine which OSCs were responsible for the observed inhibitory activities. In addition, this study delineated, in a qualitative manner, the central role that the molecular lipophilicity plays in determining the inhibitory potencies of these compounds.

In the present work, we have employed quantitative structure–activity relationship (QSAR) analysis to more critically evaluate proposed inhibitor–enzyme interactions and also provide additional guidance to directions of future molecular design for this class of compounds. The reported activity data were modeled by means of multiple regression analysis (MLR) and partial least-squares (PLS) techniques. The PLS approach is one of the most useful techniques for molecular modeling in drug design (17), and it has been successfully applied to several quantitative structure–activity and structure–property studies (18–21).

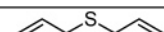
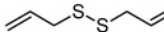
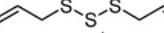
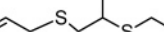
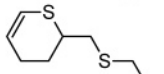
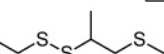
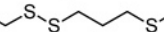

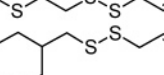


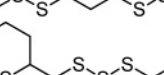

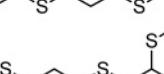

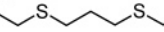
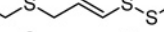


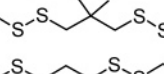

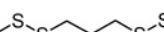
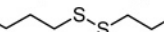

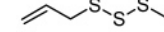

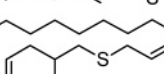
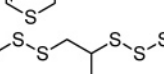
The structures of the compounds under study were characterized by means of calculated physicochemical properties and several nonempirical descriptors, such as topological, geometrical, and quantum chemical indices. The main purpose of this work was to understand in what way the different characteristics of OSCs (bulkiness, hydrophobicity, and electronic features) contribute to optimal inhibitory activity on 15-sLO.

MATERIALS AND METHODS

Biological Data. The chemical structures along with observed activity data of the compounds used in this study are shown in Table 1. The inhibitory activity data on 15-sLO were taken from Block and co-workers (16). The $\log 1/IC_{50}$ values were used as a dependent variable in which IC_{50} represents the molar concentration of compound required to achieve 50% of inhibition of 15-sLO.

Structural Descriptors. A large number of descriptors were calculated to characterize the compounds under study. Like indicators of molecular size were considered: molar volume (V_m), molecular weight (MW), and molar refractivity (MR). To explain lipophilicity effects, the octanol–water partition coefficient, as $\log P_{oct}$, was calculated by using the Interactive Analysis LogP and LogW (water solubility) predictor website. The other group of structural descriptors included several quantum chemical indices. The compound starting geometries were built in a fully extended conformation within the HyperChem package (release 7.5 for Windows). The three-dimensional molecular structures were obtained by energy minimization using the MM+ molecular mechanics potential-energy function. In a follow-up procedure, a complete optimization of the geometrical parameters was carried out by using the AM1 method implemented in the standard version of MOPAC 6.0. The following indices obtained from molecular orbital calculations were considered: total energy (E_{total}), heat of formation (ΔH_f), energy of highest occupied molecular orbital (HOMO), energy of lowest unoccupied molecular orbital (LUMO), dipole moment (μ), absolute total charge (Q_{total}), the most positive and the most negative absolute charges ($q_{p,max}$, $q_{n,max}$), and the positive and negative relative charge (RNCG, RPCG). The last group of descriptors considered in

Table 1. Soybean 15-Lipoxygenase Inhibitory Activity Data of Organosulfur Compounds

Number	Compound	IC_{50} (μM) ^a
01		1800
02		514
03		289
04		319
05		650
06		31
07		29
08		29
09		37
10		28
11		8
12		51
13		20
14		14
15		43
16		37
17		25
18		21
19		10
20		9
21		8
22		2
23		860
24		425
25		90
26		4
27		650
28		20

^a Micromolar concentration of compound required to achieve 50% of inhibition of 15-sLO.

this study included several geometrical and topological indices: the Wiener index, the valence and connectivity molecular indices, the kappa shape indices, and several geometrical indices calculated from the optimized distance matrix AM1 by using the Dragon software (v 3.0) (22).

Table 2. Molecular Descriptors^a for the Compounds Described in Table 1

compd	IC ₅₀ (μM)	Log P _{oct}	SASA	ADDD	L/Bw	PJ13	LUMO
1	1800	2.75	318.32	17.059	17.5	0.971	0.225
2	514	2.91	352.69	19.160	24.3	0.690	-1.552
3	289	3.01	393.99	20.222	7.6	0.938	-2.287
4	319	4.38	434.17	27.556	16.3	0.852	0.071
5	650	4.26	399.15	25.659	8.7	0.823	0.140
6	31	7.00	469.76	28.985	14.3	0.971	-1.596
7	29	7.27	477.78	29.494	20.3	0.813	-1.631
8	29	4.61	431.77	27.004	9.8	0.885	-1.705
9	37	4.59	426.04	26.671	11.4	0.943	-1.700
10	28	7.43	478.70	30.578	19.3	0.819	-1.815
11	8	7.98	512.93	30.687	11.6	0.852	-1.774
12	51	6.89	460.40	27.400	4.3	0.694	-2.365
13	20	8.13	529.01	31.563	10.7	0.925	-2.373
14	14	6.09	503.33	35.041	9.3	0.817	-1.691
15	43	4.42	447.26	28.167	39.1	0.999	0.291
16	37	7.31	475.32	26.864	7.8	0.637	-1.746
17	25	7.49	485.49	28.135	29.6	0.838	-1.906
18	21	6.09	483.14	30.444	13.9	0.824	-1.656
19	10	7.96	540.48	35.843	10.3	0.800	-1.638
20	9	7.56	551.25	37.921	15.9	0.947	-1.615
21	8	6.85	531.16	34.143	6.6	0.728	-1.737
22	2	8.57	598.62	39.889	21.4	0.834	-1.684
23	860	2.21	298.95	14.388	8.3	0.864	-1.575
24	425	2.27	336.86	16.157	13.1	0.802	-2.256
25	90	6.20	418.41	27.762	7.2	0.636	-1.799
26	4	7.41	539.23	44.538	81.1	0.871	3.509
27	650	4.24	395.43	25.445	8.0	0.803	0.335
28	20	8.13	524.80	30.820	7.0	0.635	-2.434

^a For explanations of the symbols of molecular descriptors, see the text.

Statistical Methods. Multiple regression analysis (MLR) and partial least-squares projections in latent variables (PLS) were the methods used to search for relationships between the biological activity data and the structural descriptors. PLS is a projection method that relates the information in the response matrix *Y* to the systematic variation in the descriptor matrix *X*. It can analyze data with strongly collinear, noisy, and numerous *X* variables, and the determination of the significant number of PLS components is carried out by cross-validation. From the PLS loadings it is possible to evaluate the influence of each descriptor variable to the modeling of the biological activity under study. PLS analysis was carried out using the SIMCA-P 7.01 software package obtained from Umetri AB, Umea, Sweden, and MLR analysis was performed by using the 7.0 version of Statgraphics Plus software.

RESULTS AND DISCUSSION

Multiple Regression Analysis. MLR was performed on compounds 1–28 described in Table 1, whereas Table 2 lists the molecular descriptors included in the selected models. Because of the large number of descriptors considered, a stepwise multiple regression procedure based on the forward-selection and backward-elimination methods was used for inclusion or rejection of descriptors in the screened models. To avoid overestimations or difficulties in interpretation of the resulting models, pairs of variables with an *r* ≥ 0.75 were classified as intercorrelating ones, and only one of these was included in the screened model. After some consideration, the following equations were selected:

$$\log 1/IC_{50} = 2.366 (0.237) + 0.330 (0.038) \log P_{oct} \quad (1)$$

$$R^2 = 0.742; R^2(cv) = 0.704; s = 0.401; n = 28; F = 74.60; W_{\log P_{oct}} = 2.102$$

$$\log 1/IC_{50} = -0.146 (0.329) + 0.0097 (0.0007) SASA \quad (2)$$

$$R^2 = 0.878; R^2(cv) = 0.859; s = 0.276; n = 28; F = 186.60; W_{SASA} = 2.912$$

In these and the following equations, *n* is the number of compounds, *s* is the standard deviation, *R*² is the squared correlation coefficient, *R*²(cv) is the squared cross-validation coefficient, and *F* is the Fisher *F* statistic. The figures in parentheses are the standard deviations and *P* values of coefficients, and *W* is the standardized regression coefficient obtained when the variables are scaled to the same numerical range (0–1). The statistical quality of eq 1 is good, and although a moderate correlation was found between log *P*_{oct} and log 1/*IC*₅₀, it suggests that the molecular lipophilicity plays an important role in 15-sLO inhibition. An interesting point to highlight is the lower level of statistical significance that is obtained when other calculated log *P*_{oct} parameters were used to derive this equation. A better fit, however, was found by using a parameter related to molecular size such as the solvent-accessible surface area (SASA), as shown in eq 2. The standard deviation as well as the fitting and predictive capabilities expressed by *R*² and *R*²(cv), respectively, are clearly better, and the agreement between the observed and calculated values is very satisfactory. The positive dependence of log 1/*IC*₅₀ on SASA reflects the decisive role played by the nonspecific van der Waals interactions in the 15-sLO inhibitory potency of considered compounds. Thus, by analyzing both equations, one can conclude that the greater lipophilicity or molecular size (as reflected by SASA), the greater will be the inhibitory effectiveness of the compounds under study. However, although one may conjecture that both molecular factors are of prime importance, they are not enough to explain completely the inhibitory activity displayed for these compounds, which is made evident by the following equations:

$$\log 1/IC_{50} = -0.250 (0.284) + 0.0088 (0.00066) SASA - 0.176 (0.057) LUMO + 0.0164 (0.005) L/Bw \quad (3)$$

$$R^2 = 0.918; R^2(cv) = 0.869; s = 0.236; n = 28; F = 89.02$$

$$W_{SASA} = 2.657; W_{LUMO} = -1.049; W_{L/Bw} = 1.263$$

$$\log 1/IC_{50} = -0.785 (0.206) + 0.0979 (0.0067) ADDD - 0.344 (0.051) LUMO + 0.0175 (0.0046) L/Bw \quad (4)$$

$$R^2 = 0.928; R^2(cv) = 0.907; s = 0.220; n = 28; F = 102.77$$

$$W_{ADDD} = 2.952; W_{LUMO} = -2.049; W_{L/Bw} = 1.349$$

Both equations are highly significant statistically, and there are no strong intercorrelations among the parameters included, which is fundamental to reach a correct physicochemical interpretation. The *r* values between pairs of descriptors were as follows: SASA/LUMO, 0.06; LUMO/L/Bw, 0.75; SASA/L/Bw, 0.20; ADDD/LUMO, 0.23; and ADDD/L/Bw, 0.40. The

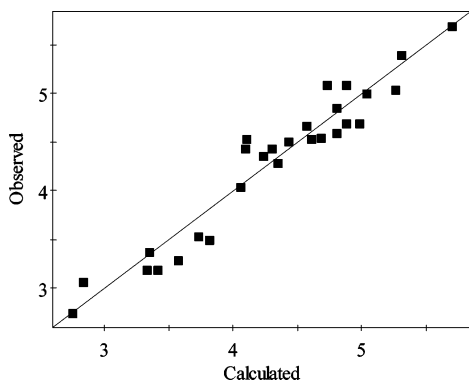


Figure 1. Relationships between the experimental and calculated inhibitory activities of all compounds shown in **Table 1** by using PLS model 1.

evaluation of the descriptor weights (W) for these equations shows that primarily the two terms related to the molecular size (SASA and ADDD) followed by the LUMO descriptor make the highest contributions to the variation in $\log 1/IC_{50}$. The significant contribution of the LUMO term in both equations is especially promising because it agrees very well with the catalytic mechanism of the 15-sLO reaction recently proposed by Ruddat and co-workers (23). The authors, by using site-directed mutagenesis techniques and steady-state and stopped-flow kinetics, demonstrated that within the catalytic domain of 15-sLO, the tryptophan amino acid at position 500 is one of the critical residues for the enzyme–substrate binding. As

mentioned, eq 3 or 4 agrees very well with such a finding, because the LUMO term suggests that the inhibitory activity on 15-sLO is strongly dependent on the interaction between an electron-acceptor compound and a nucleophilic group present in the 15-sLO molecule. Thus, taking into account that tryptophan is the most effective π -electron donor among the four fundamental aromatic amino acids which enter into the constitution of proteins (phenylalanine, tyrosine, histidine, and tryptophan) (24), it is apparent from the obtained equations that lower LUMO energy of organosulfur compound will generally result in a stronger electron donor–acceptor interaction with tryptophan⁵⁰⁰ and, therefore, in a higher inhibitory potency.

On the other hand, the presence of the length-to-breadth ratio parameter (L/Bw) in both equations suggests a lower but still highly significant influence of the molecular shape in the enzyme–inhibitor binding. Thus, the more elongated molecules will have a higher L/Bw value and will consequently interact more strongly at the enzyme-binding site. This is in agreement with the findings by other authors (9) who have shown that the binding site of 15-sLO can accommodate C18 and C20 substrate fatty acids in relatively extended conformations but cannot accommodate their U-shaped conformations. This view is consistent with the positive coefficient of L/Bw , which reflects the importance of the molecular linearity in the enzyme–inhibitor binding. Furthermore, it is possible that the U-shaped conformation of inhibitor does not allow the compounds to interact well with the hydrophobic space of the ligand binding pocket.

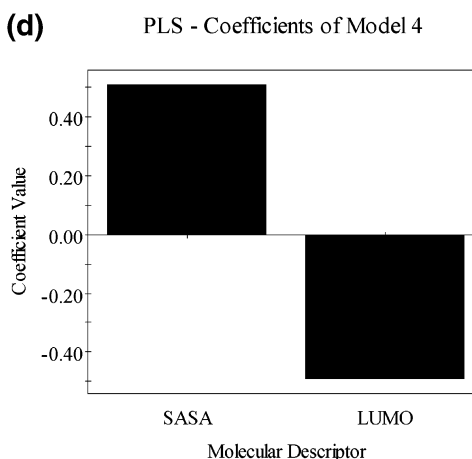
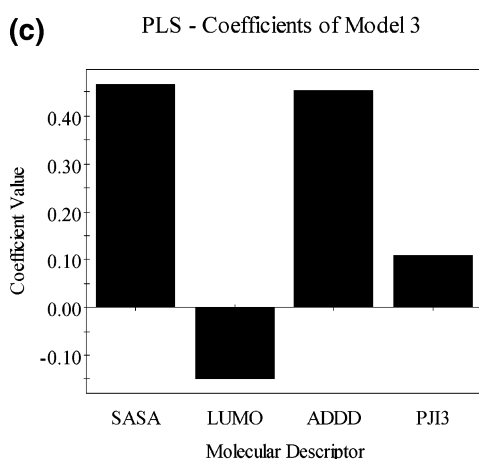
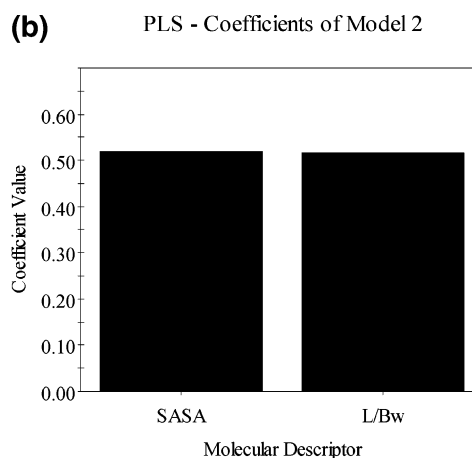
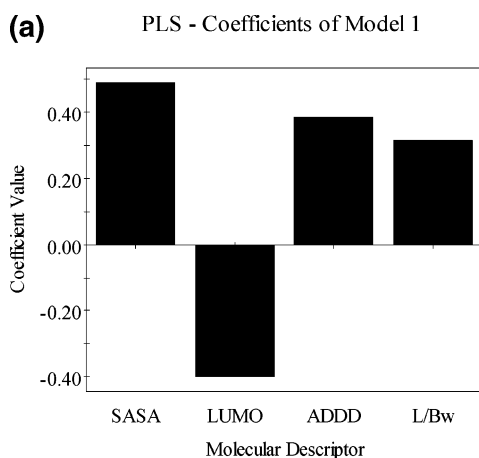


Figure 2. Comparison of PLS regression coefficients for the four developed PLS models: (a) M1 model based on all compounds considered in this study; (b) M2 model including only the five sulfides and tetradecane; (c) M3 model and (d) M4 model, based on di- and trisulfides, respectively. The molecular descriptors used in all models are listed in **Table 2**.

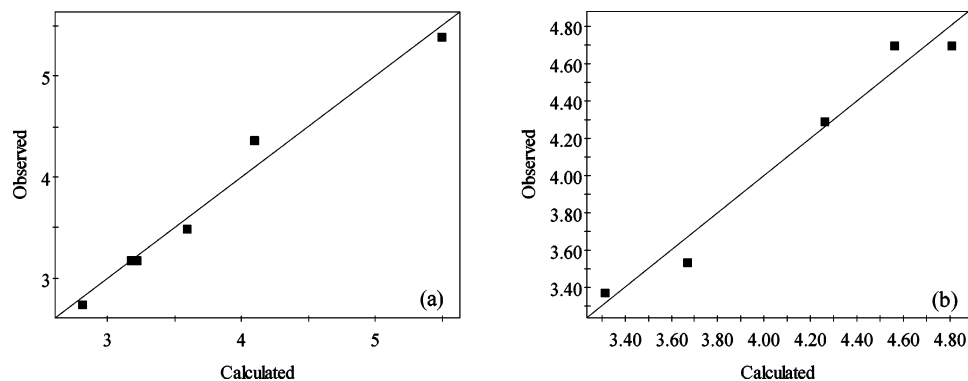


Figure 3. Relationships between the experimental and calculated $\log 1/IC_{50}$ values for 15-sLO: (a) model 2; (b) model 4.

Finally, the average distance/distance degree descriptor (ADDD) included in eq 4 encodes information about the molecular size, which can be evidenced by the collinearity exhibited between SASA and ADDD ($r = 0.93$) or V_m and ADDD ($r = 0.96$). However, a careful examination of the ADDD values shows that the discrimination among compounds produced by this index is not based entirely on size but also on other structural factors such as the molecular folding. Thus, the ADDD index quantifies this factor and shows that a greater folding degree of the organosulfur compound will result in a lower value of the ADDD index, and, consequently, a detrimental effect on its inhibitory activity will be observed. Thus, from a structural point of view, this fact provides additional support to the above-mentioned analysis on the L/Bw parameter.

PLS Regression Analysis. All variables used in the PLS calculations were initially autoscaled to zero mean and unit variance to give each descriptor equal importance in the PLS analysis. The statistical significance of the screened models was judged by the parameters already mentioned. The predictive ability was evaluated by the cross-validation coefficient (Q^2), which is based on the prediction error sum of squares (PRESS). The PRESS statistic is computed as the squared differences between observed and predicted values when the observations are kept out of the derived model. This procedure is repeated several times until every observation has been kept out once and only once. Preliminary analysis of the different PLS models performed on the whole series of compounds showed that the most important variables were those which had been useful in the regression analysis.

To explore the possibility that compounds in the data set may interact with the 15-sLO differently, the PLS study was organized in the following way: first, to obtain a general model using the variables selected in the MLR analysis and, second, to derive correlation models for each of the classes of OSCs here studied; that is, compounds with a $-S-$, $-SS-$, or $-SSS-$ functional group in their molecular structure. The objective of constructing PLS models for the members of each group was to determine if additional information is captured by the subset models, as compared to the general model.

The first model (M1) was performed on the 28 compounds shown in Table 1, and the descriptor matrix consisted of the same variables as used in eqs 3 and 4. The PLS analysis resulted in a significant three-component model with the following statistics: $R^2 = 0.931$, $Q^2 = 0.907$, $s = 0.216$, $n = 28$, and $F = 107.95$. A comparison of the quality between the obtained model and eqs 3–4 shows that the PLS model has a similar data-fitting/predictive ability at a high level of significance. As can be seen in Figure 1, the agreement between measured and calculated data is very satisfactory. Figure 2a shows the selected

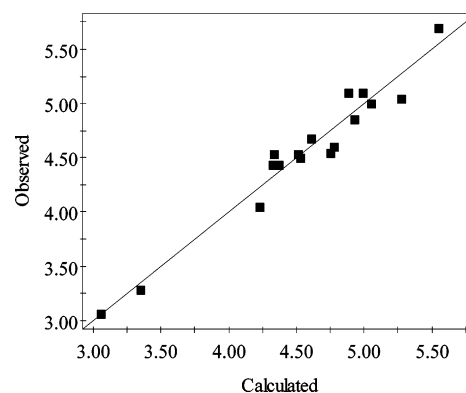


Figure 4. Relationships between the experimental and calculated inhibitory activity of 17 disulfides shown in Table 1 by using PLS model 3.

descriptors and the corresponding PLS pseudo-regression coefficients. According to these values, it can be inferred that, as expected, the size and molecular shape as well as the solute's electron-acceptor capacity play a predominant role in the inhibitory activity exhibited for these compounds.

The second model (M2) was performed only for the five sulfides and the *n*-alkane shown in Table 1, that is, compounds 1, 4, 5, 15, 26, and 27, respectively. The PLS analysis resulted in a significant one-component model with the following statistics: $R^2 = 0.980$, $Q^2 = 0.966$, $s = 0.155$, $n = 6$, and $F = 194.58$. The relationship between the measured $\log 1/IC_{50}$ data and values calculated by the model is illustrated in Figure 3a. Only two predictor variables, SASA and L/Bw, were necessary to describe the inhibitory activity of these compounds. Because both descriptors are related with the size and molecular shape, it can be concluded that for this class of compounds, $\log 1/IC_{50}$ is mainly governed by intermolecular dispersive interactions at the enzyme-binding site. An interesting point to highlight is that the HOMO parameter, which reflects the solute's electron-donor capacity, is not seen to be important for the inhibitory activity of the monosulfides under study. However, taking into account the limited amount of monosulfides studied, the influence of HOMO energy cannot be ruled out on the basis of only this analyzed subset and, therefore, further work is needed to obtain a full understanding of the interaction between the monosulfides and the 15-sLO. Figure 2b shows the selected descriptors and the corresponding PLS pseudo-regression coefficients. According to these values, sulfides with great molecular size or a high degree of molecular linearity will have high values of SASA and L/Bw, respectively, and consequently, it will interact more strongly at the enzyme-binding site.

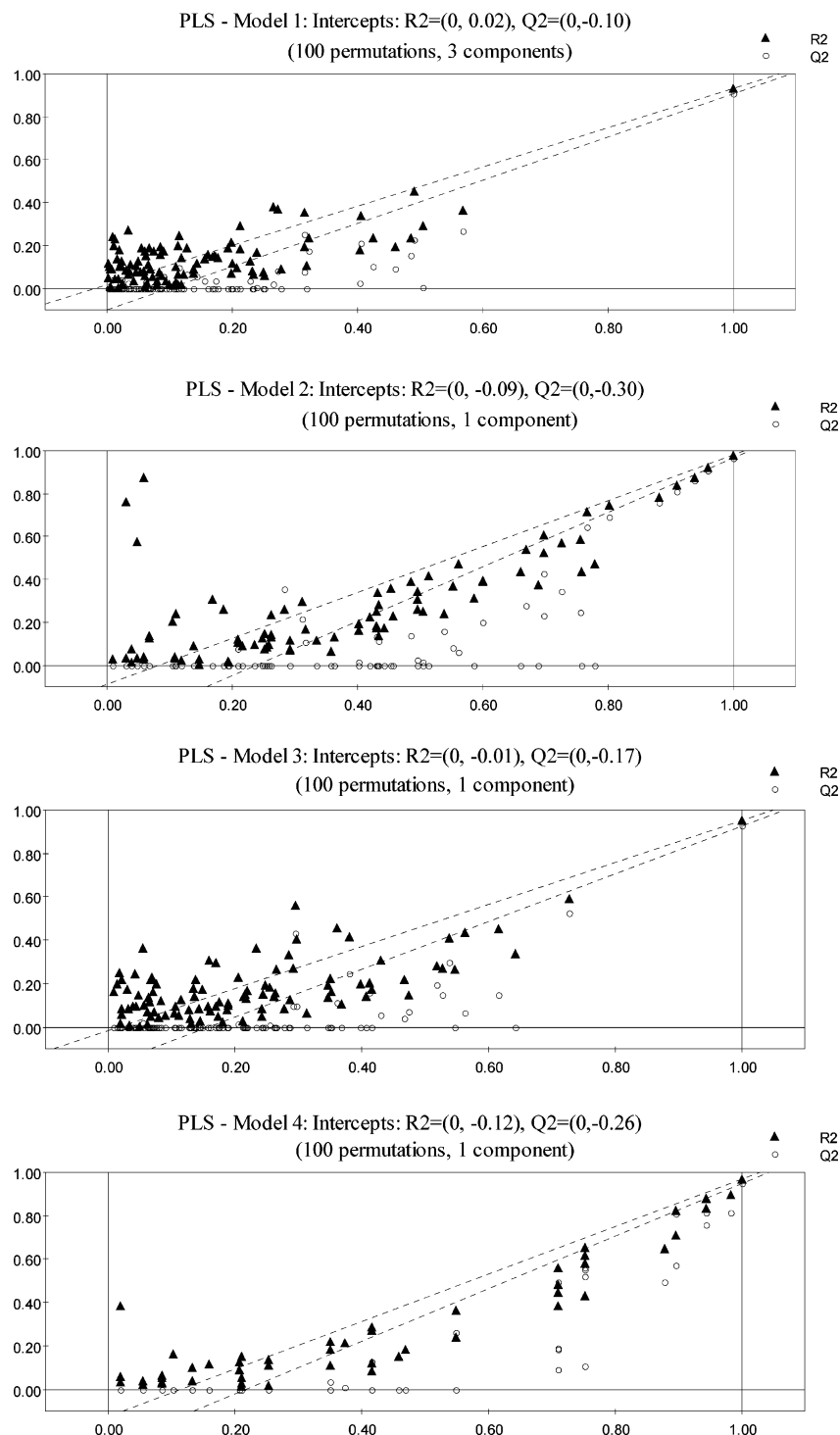


Figure 5. Results of the permutation test. The R^2 and Q^2 values were obtained from 100 permutations for the four developed PLS models.

The third model (M3) was performed on the 17 compounds that have a disulfide functional group in their structure. The PLS analysis resulted in a highly significant one-component model with the following statistics: $R^2 = 0.952$, $Q^2 = 0.926$, $s = 0.144$, $n = 17$, and $F = 298.42$. The quality of the derived model may also be demonstrated by direct comparison between the experimental and calculated activities given in Figure 4. The selected descriptors and their corresponding PLS pseudo-regression coefficients are shown in Figure 2c. Inspection of these values reveals that the SASA and ADDD bulkiness parameters have the highest weights followed by LUMO and the three-dimensional Petitjean shape index (PJI3). On this basis,

one may conjecture that the nonspecific intermolecular dispersive interactions are of prime importance for the inhibitory activity of the disulfides under study, whereas the differences in molecular shape as well as the electron pair donor–acceptor interactions are also involved but are not dominant.

Finally, in the fourth model (M4), which was performed on those compounds with a trisulfide functional group in their structure (compounds 3, 12, 13, 24, and 28), one significant PLS component was obtained with the following statistics: $R^2 = 0.973$, $Q^2 = 0.958$, $s = 0.119$, $n = 5$, and $F = 109.30$. The agreement between the observed and calculated values is very good, as shown in Figure 3b. This component was relevant

principally with two molecular structural descriptors, ADDD and LUMO. The high R^2x value of this PLS model (0.970) implies that these variables are intercorrelated for the data points analyzed ($r = 0.940$), which limits the applicability of MLR analysis. Even though this model is based on too small a number of data points, both structural parameters are highly significant statistically and clearly show that the inhibitory activity of trisulfides analogues strongly depends on the electron-acceptor capacity of the S—S—S bond as well as on the size and molecular shape as reflected by the LUMO and ADDD indices, respectively. The PLS pseudo-regression coefficients shown in **Figure 2d** support the above-mentioned analysis.

In summary, the developed QSAR models on garlic oil components and homologues show the principal factors that govern the inhibitory activities of these compounds. The positive dependence of $\log 1/IC_{50}$ on SASA or ADDD in all models reflects the fundamental role that the nonspecific van der Waals interactions play in the 15-sLO inhibitory potency of considered compounds. On the other hand, the developed models provided additional support for the hypothesis of an electron-acceptor role for OSCs in the inhibitor–enzyme complex. Furthermore, as illustrated by **Figure 2**, the ability of these compounds to participate in electron pair donor–acceptor interactions is particularly favorable for disulfides and trisulfides, as revealed by the high contribution of the LUMO term in PLS models 3 and 4, respectively. On the other hand, it should be noted that the above observations on the bulkiness and electronic parameters does not imply that they are the sole factors in determining the inhibitory activity of the OSCs under study. Thus, geometric features as expressed by the shape parameters used in the developed QSAR models must also be taken into account, and consequently, the overall activity of a molecule at the enzyme-binding site will be determined by the detailed balance of these effects.

Model Validation. It is well-known that the real predictive ability of any QSAR model cannot be judged solely by using internal validation techniques such as cross-validation. Thus, the validity of the PLS models was additionally tested by a permutation test (25). Models were recalculated for randomly reordered response data ($\log 1/IC_{50}$). These permuted $\log 1/IC_{50}$ values were related to intact predictor data by refitting the model and including cross-validation. When R^2 and Q^2 were plotted as a function of the correlation coefficient between the original values and the predicted values, the intercept with the Y axis expressed to which degree these values rely on chance. **Figure 5** shows the results obtained from 100 permutations for each of the compounds under study. The intercepts of the two regression lines (for R^2 and Q^2) indicate the degree of overfit and overprediction. In general, intercept limits for R^2 and Q^2 of ≤ 0.30 indicate valid models, as is the case for the four PLS models here developed.

LITERATURE CITED

- (1) Solomon, E. I.; Zhou, J.; Neese, F.; Pavel, E. G. New insights from spectroscopy into the structure/function relationships of lipoxygenases. *Chem. Biol.* **1997**, *4*, 795–808.
- (2) Brash, A. R. Lipoxygenases: occurrence, functions, catalysis, and acquisition of substrate. *J. Biol. Chem.* **1999**, *274*, 23679–23682.
- (3) Roberts, L. J., II. Introduction: lipids as regulators of cell function. *Cell. Mol. Life Sci.* **2002**, *59*, 727–728.
- (4) Samuelsson, B.; Dahlen, S. E.; Lindgren, J. A.; Rouzer, C. A.; Serhan, C. N. Leukotrienes and lipoxins: structures, biosynthesis, and biological effects. *Science* **1987**, *237*, 1171–1176.
- (5) Dailey, L. A.; Imming, P. 12-Lipoxygenase: classification, possible therapeutic benefits from inhibition, and inhibitors. *Curr. Med. Chem.* **1999**, *6*, 389–398.
- (6) Ding, X. Z.; Tong, W. G.; Adrian, T. E. Cyclooxygenases and lipoxygenases as potential targets for treatment of pancreatic cancer. *Pancreatol.* **2001**, *1*, 291–299.
- (7) Cornicelli, J. A.; Trivedi, B. K. 15-Lipoxygenase and its inhibition: a novel therapeutic target for vascular disease. *Curr. Pharm. Des.* **1999**, *5*, 11–20.
- (8) Steinberg, D.; Parthasarathy, S.; Carew, T. E.; Khoo, J. C.; Witztum, J. L. Modifications of low-density lipoprotein that increase its atherogenicity. *N. Engl. J. Med.* **1989**, *320*, 915–924.
- (9) Minor, W.; Steczko, J.; Stec, B.; Otwinowski, Z.; Bolin, J. T.; Walter, R.; Axelrod, B. Crystal structure of soybean lipoxygenase L-1 at 1.4 Å resolution. *Biochemistry* **1996**, *35*, 10687–10701.
- (10) Kuhn, H.; Saam, J.; Eibach, S.; Holzthutter, H. G.; Ivanov, I.; Walther, M. Structural biology of mammalian lipoxygenases: enzymatic consequences of targeted alterations of the protein structure. *Biochem. Biophys. Res. Commun.* **2005**, *338*, 93–101.
- (11) Pontiki, E.; Hadjipavlou-Litina, D. Lipoxygenases (LOs): a heterogenous family of lipid peroxidizing enzymes implicated in cell differentiation, inflammation, asthma, carcinogenesis, atherogenesis—an interesting target for the development of promising drugs. *Curr. Enzyme Inhib.* **2005**, *1*, 309–327.
- (12) Rabinowitch, H. D., Currah, L., Eds. Health and alliums. In *Allium Crop Science: Recent Advances*; CAB International: Wallingford, U.K., 2002; 515 pp.
- (13) Camargo, A. B.; Masuelli, R. W.; Burba, J. L. Characterization of Argentine garlic cultivars for their allicin content. *Acta Hort.* **2005**, *688*, 309–312.
- (14) Tapiero, H.; Townsend, D.; Tew, K. Organosulfur compounds from alliaceae in the prevention of human pathologies. *Biomed. Pharmacother.* **2004**, *58*, 183–193.
- (15) Sing, U.; Prithiviraj, B.; Sarma, B. K.; Sing, M.; Ray, A. B. Role of garlic (*Allium sativum* L.) in human and plant diseases. *Indian J. Exp. Biol.* **2001**, *39*, 310–322.
- (16) Block, E.; Iyer, R.; Grisoni, S.; Saha, C.; Belman, S.; Lossing, F. P. Lipoxygenase inhibitors from the essential oil of garlic. Markovnikov addition of the allyldithio radical to olefins. *J. Am. Chem. Soc.* **1988**, *110*, 7813–7827.
- (17) Wold, S. PLS for multivariate linear modeling. In *Chemometric Methods in Molecular Design*; Van de Waterbeemd, H., Ed.; Wiley-VCH: Weinheim, Germany, 1995; Vol. 2, pp 195–218.
- (18) Luco, J. M. Prediction of brain–blood distribution of a large set of drugs from structurally-derived descriptors using partial least squares (PLS) modeling. *J. Chem. Inf. Comput. Sci.* **1999**, *39*, 396–404.
- (19) Silva, M. F.; Chipre, L. F.; Raba, J.; Luco, J. M. Amino acids characterization by reversed-phase liquid chromatography. Partial least-squares modeling of their transport properties. *Chromatographia* **2001**, *53*, 392–400.
- (20) Luco, J. M.; Salinas, A. P.; Torriero, A. A. J.; Vazquez, R. N.; Raba, J.; Marchevsky, E. J. Immobilized artificial membrane chromatography: quantitative structure–retention relationships of structurally diverse drugs. *J. Chem. Inf. Comput. Sci.* **2003**, *43*, 2129–2136.
- (21) Luco, J. M.; Marchevsky, E.; QSAR Studies on blood–brain barrier permeation. *Curr. Comput.-Aided Drug Design* **2006**, *2*, 31–55.
- (22) Todeschini, R.; Consonni, V. In *Handbook of Molecular Descriptors*; Mannhold, R., Kubinyi, H., Timmerman, H., Eds.; Wiley-VCH: Weinheim, Germany, 2000; Vol. 11, pp 1–667.

- (23) Ruddat, V. C.; Mogul, R.; Chorny, I.; Chen, C.; Perrin, N.; Whitman, S.; Kenyon, V.; Jacobson, M. P.; Bernasconi, C. F.; Holman, T. R. Tryptophan 500 and arginine 707 define product and substrate active site binding in soybean lipoxygenase-1. *Biochemistry* **2004**, *43*, 13063–13071.
- (24) Pullman, B.; Pullman, A. Electron-donor and acceptor properties of biologically important purines, pyrimidines, pteridines, flavins, and aromatic amino acids. *Proc. Natl. Acad. Sci. U.S.A.* **1958**, *44*, 1197–1202.
- (25) Eriksson, L.; Johansson, E.; Muller, M.; Wold, S. Cluster-based design in environmental QSAR. *Quant. Struct.–Act. Relat.* **1997**, *16*, 383–390.

Received for review October 20, 2006. Revised manuscript received January 2, 2007. Accepted January 3, 2007. The present work was supported by grants from the University of San Luis and CONICET, Argentina.

JF063020E